

# Placement and Power Assignment for Hierarchical UAV Networks under Hovering Fluctuations in mmWave Communications

Mehran Pourmohammad Abdollahi<sup>1</sup>, Hosein Azarhava<sup>1</sup>, and Javad Musevi Niya<sup>1</sup>

<sup>1</sup>University of Tabriz Faculty of Electrical and Computer Engineering

June 1, 2023

## Abstract

In this paper, we investigate the successful transmission probability of an aerial cellular network in which an unmanned aerial vehicle (UAV) as a Macrocell Base Station (UAV-BS) serves other UAVs as aerial users. The beamforming capable antennas are mounted on the UAVs, to increase the throughput of the network. The random effects of inner forces such as controlling errors or outer forces like the air conditions result in the random fluctuations. We assume Rician fading distribution over the links between the UAVs, then, we calculate the distribution of the channels under hovering fluctuations. Also, we derive the closed form expressions for successful transmission probability. Defining an optimization problem on the average successful transmission probability of the network, we obtain the best placement of UAV-BS along with the resource allocation. The problem turns out to be a non-convex problem and time consuming via numerical exhaustive search methods. Instead, we solve the optimization problem for its lower bound. Maximization problem for the achieved lower bound is equivalent to maximize the main problem. Then, we use some approximations to convert it to a low complex problem to find the solution. We use the entity of the low complex problem to obtain the allocated power for each UAV and in the following, the problem becomes convex which is solved by KKT conditions to obtain the location of UAV-BS. The theoretical results show that optimizing the lower bound probability achieves the suboptimal solution for power assignment and placement problem, which is verified by simulation results.

**RESEARCH**

# Placement and Power Assignment for Hierarchical UAV Networks under Hovering Fluctuations in mmWave Communications

Hosein Azarhava<sup>1</sup> | Mehran Pourmohammad Abdollahi<sup>\*2</sup> | Javad Musevi Niya<sup>3</sup><sup>1</sup>Faculty of Electrical and Computer Engineering, University of Tabriz, East Azarbayjan, Iran<sup>2</sup>Faculty of Electrical and Computer Engineering, University of Tabriz, East Azarbayjan, Iran<sup>3</sup>Faculty of Electrical and Computer Engineering, University of Tabriz, East Azarbayjan, Iran**Correspondence**

\*Mehran Pourmohammad Abdollahi,  
Faculty of Computer and Electrical  
Engineering, University of Tabriz, East  
Azarbayjan, Iran. Email:  
mehran.pour@tabrizu.ac.ir

**Abstract**

In this paper, we investigate the successful transmission probability of an aerial cellular network in which an unmanned aerial vehicle (UAV) as a Macrocell Base Station (UAV-BS) serves other UAVs as aerial users. The beamforming capable antennas are mounted on the UAVs, to increase the throughput of the network. The random effects of inner forces such as controlling errors or outer forces like the air conditions result in the random fluctuations. We assume Rician fading distribution over the links between the UAVs, then, we calculate the distribution of the channels under hovering fluctuations. Also, we derive the closed form expressions for successful transmission probability. Defining an optimization problem on the average successful transmission probability of the network, we obtain the best placement of UAV-BS along with the resource allocation. The problem turns out to be a non-convex problem and time consuming via numerical exhaustive search methods. Instead, we solve the optimization problem for its lower bound. Maximization problem for the achieved lower bound is equivalent to maximize the main problem. Then, we use some approximations to convert it to a low complex problem to find the solution. We use the entity of the low complex problem to obtain the allocated power for each UAV and in the following, the problem becomes convex which is solved by KKT conditions to obtain the location of UAV-BS. The theoretical results show that optimizing the lower bound probability achieves the suboptimal solution for power assignment and placement problem, which is verified by simulation results.

**KEYWORDS:**

Hierarchical UAV Network, successful transmission probability, mmWave communications, antenna array, UAV fluctuation

## 1 | INTRODUCTION

The emerging Unmanned Aerial Vehicle (UAV) technology has attracted a great research interest whether in industrial areas such as providing logistic applications or telecommunication projects specially in 5G networks such as monitoring devices, aerial base stations, aerial users and etc. Attaching the UAVs to the cellular networks could enhance its performance and provide more qualified services. Particularly, the flexibility for adjusting altitude (generally the location), has become a privilege in proportion to the terrestrial base stations which enables them to increase the Line-of-Sight (LoS) probability<sup>1</sup> to the ground users. However, the increasing demand to apply multiple UAVs has created great challenges such as coverage probability, link capacity, channel

model analysis and etc. in 5G communications. To provide a network infrastructure for a large number of mobile users and Internet of Things (IoT) devices and to extend the coverage of terrestrial base stations specially to remote areas, the architectures, requirements and corresponding issues of integrating UAVs with such networks have been widely discussed in<sup>2,3,4,5</sup>.

## 1.1 | Related Works

The deployment of UAVs in swarm networks was considered as flying ad hoc networks (FANETs) or Internet of Drones (IoD) which enhance the Quality of Experience (QoE) for ground terminals<sup>6</sup>. A multi-antenna UAV was considered to communicate with a cluster of single-antenna IoT devices as a MIMO link and the data collection efficiency was optimized over the transmission power parameter during the whole flight time<sup>7</sup>. On the contrary, the joint trajectory and achievable sum rate of UAV-assisted IoT networks in downlink direction, were achieved using an efficient iterative algorithm which optimizes the power allocation in the network<sup>8</sup>. In traditional methods, the gathered data from wireless sensors is recorded during the flight of a UAV and is offloaded at the end of the journey. Due to high data rate and low delay in 5G networks, the UAVs could make use of transmissions during their flight which lowers the risk of data loss. However, the performance of 5G networks is highly dependent on the channel statuses, obstacles and movements of the UAVs. Therefore, an integrated full-stack simulation framework was proposed to evaluate the end-to-end data transfer in the network for mmWave communications which decreases the data loss during flight time<sup>9</sup>. Likewise, an Intelligent UAV-based Data Aggregation Algorithm, (IDAA) was proposed in which the security tasks are done in the UAVs and an energy efficient trajectory is planned by deep reinforcement learning methods to collect more data by UAVs<sup>10</sup>. Intell-UAV-5G was proposed to predict the connected access nodes and intelligently provide the service in 5G networks. Minimizing the time of service interruption, the Intell-UAV-5G algorithm guarantees the quality of service and outperforms the existing methods<sup>11</sup>. Z. Ullah *et al.* classified the joint optimization problems for UAV networks based on the various parameters and they have shown the effect of similar learning methods such as artificial intelligence (AI), machine learning (ML), deep reinforcement learning (DRL), mobile edge computing (MEC) and software-defined networks (SDN) on solving the problems<sup>12</sup>. H. Bian *et al.* utilized an iterative algorithm to optimize the trajectory and power allocation for a UAV-assisted vehicular network over movement and information-causality constraints and they showed the effect of UAV's cache in performance of the network<sup>13</sup>. A height dependent channel model and antenna patterns were taken to account to evaluate the coverage probability and rate of both links in which the overlay method seems to show better performance. The study on impact of realistic channel models in such networks showed that the power control policy could be useful to find the best performance trade-off for both U2U and GU communications<sup>14</sup>. An efficient beam tracking was proposed using a beam training method to predict the beam direction of a UAV base station which communicates with mobile users<sup>15</sup>. The beam training codebook design was considered for both insufficient and sufficient beam training cases which increases the average downlink capacity of the network in compared with the other conventional methods. A multi-antenna UAV was deployed to cover a set of ground base stations in which the line of sight phenomenon and ground base stations' interference in uplink mode could be considered as a challenge in maximizing the uplink sumrate<sup>16</sup>.

The dynamic model for the flock of UAVs was investigated to obtain the efficient trajectory planning via Improved Particle Swarm Optimization (IPSO) and Gauss Pseudo-spectral Method (GPM)<sup>17</sup>. Also, a hierarchical exploitation of swarm UAVs was studied for a reliable communication with ground base stations (GBSs) and a new protocol was introduced via choosing a swarm head among the UAVs to overcome the interference of occupied GBSs<sup>18</sup>. A cooperative UAV sense-and-send protocol was proposed for UAV-to-X communications in the uplink to optimize joint subchannel and speed in multi-UAV networks<sup>19</sup>. The spectrum sharing was considered in UAV networks where both U2U pairs and Ground Users (GUs) could transmit their signals in underlay or overlay mode resulting a mutual interference<sup>20</sup>. In a cellular network with multiple UAVs, the average capacity of the link between each UAV and its ground users was maximized simultaneously, guaranteeing the overall area coverage<sup>21</sup>. Turning angle constraint was considered in UAV-to-UAV (U2U) communications and an energy optimization problem was defined over joint UAV flight path planning and transmit power control which results in shortening the completion time length<sup>22</sup>. Likewise, the 3D movement of the UAVs with fix velocities were investigated to simulate the wideband non-stationary Air-to-Air (A2A) channel model in which the results show that the impact of vertical movements is larger than horizontal movements<sup>23</sup>. X. Duan *et al.* employed the (UAV)-enabled wireless power transfer (WPT) to transmit energy to ground users with lower energy levels. The authors jointly optimized the three-dimensional (3D) location of UAV and beam pattern by applying the Butler Matrix feed network which maximizes the energy harvesting gain in the network<sup>24</sup>. C. T. Cicek *et al.* investigated the optimum location of several Drone Base Stations (DBSs) with dynamic capacity which serve their ground users in a cellular network. The authors showed that the capacity of each DBS is a non-linear function of distance and resources received from ground base stations which

resulted in a Mixed Integer Non-Linear Program (MINLP) and was solved through heuristical methods<sup>25</sup>. F. Xu *et al.* proposed an improved mean shift (IMS) algorithm to find the optimum location of UAVs where they provide computing services for the ground users. They showed the trade-off between the cost of service providers and energy consumption in such networks<sup>26</sup>. An adaptive discrete particle swarm optimization (ADPSO) algorithm and power calibration were employed to optimally localize the UAVs in order to minimize the security threats of other UAVs<sup>27</sup>. Also, deployment of UAVs as helpers to the main base station was investigated by V. Sharma *et al.*<sup>28</sup> in which a self-healing neural model and the concept of matrix-coloring have been proposed to maximize the UAVs positioning likelihood which optimizes the throughput of the network. On the other hand, a self-healing mechanism in MAC layer and a fast beam tracking mechanism were developed to repair the failed links and maximize the robustness of the UAV mesh networks<sup>29</sup>. An optimal energy-saving algorithm was deployed in UAV swarm networks considering the jointly balancing heterogeneous UAVs' flying distances on the ground and final service altitudes in the sky under No-Fly-Zone (NFZ) constraint and different initial locations<sup>30</sup>.

Many efforts have been made to characterize the channel models between UAVs and other user either ground or aerial users. But the mobility and hovering as the inseparable characteristics of the UAVs, make them vulnerable to fluctuating effects which reduces the antenna gains in the users with beamforming capabilities. The effects of these fluctuations as a normal random variable was applied to the problem to derive mathematical expressions for probability density function (PDF) corresponding to the channel behavior under Gamma fading<sup>31</sup>. A summary of related works is represented in Table 1.

## 1.2 | Scope and Contributions

In this paper, we consider a UAV cellular network with one aerial base station and many aerial users in which the orthogonal channels have been assigned to the users. We use the method studied in<sup>31</sup> for aerial channel modeling to evaluate the average successful transmission under Rician fading for Line-of-Sight (LoS) links. Then, we define the optimization problem to maximize the average successful transmission probability which turns out to be a non-convex problem. Using some approximations and converting the main problem to equivalent problems, we simplify the problems with lower complexity to find the closed-form expressions. Our contribution is as following:

- Considering multi UAV network communicating with a multi-antenna UAV base station, we calculate the PDF of the channel gains under UAV's hovering fluctuations over Rician fading channels.
- We derive the closed-form expression for the average successful transmission probability in the network corresponding to the location of each UAV and its allocated power.
- A tight lower bound is calculated for the average successful transmission probability of the network.
- An optimization problem is defined to maximize the average successful transmission probability over placement of the UAV base station and UAV users' transmission power. Due to the non-convexity of the defined problem, we use some approximations to convert it into a minimization problem. Finding the solution to the power allocation, we convert the problem into a convex problem which can be solved with KKT conditions resulting in the closed-form expression for location of UAV base station.

The rest of this paper is organized as follows: Section II discusses the system model of hierarchical aerial cellular network and successful transmission analysis. In section III the maximization problem is expressed to maximize the successful transmission probability. The numerical results are presented in section IV, and finally, Section V concludes the paper.

## 2 | SYSTEM MODEL

We consider a hierarchical aerial communication network shown in Figure 1 in which a UAV, as an aerial Base Station (UAV-BS), communicates with other UAV users denoted by  $U_l$  for ( $l = 1, 2, \dots, L$ ) in downlink mode. The location of UAV-BS and each  $U_l$  are given by  $(x, y, z)$  and  $(x_l, y_l, z_l)$  in Cartesian coordination, respectively. These locations are available at UAV-BS. All UAVs use rotary wings so that they could hover in the appropriate locations for the given purposes. Also, it is assumed that all UAVs are capable of beamforming since they use mmWave antennas in their receiving and transmission directions. The UAV-BS is equipped with multiple antennas so that each of them could be aligned towards the aerial users, independently.

**Table 1** Summary of Relevant Articles

Main Subject	Perf. Analysis	Optimization	Fluctuation	Multi UAV	Ref.
Sum-rate optimization in UAV-aided MIMO communications	×	✓	×	×	7
Trajectory and power optimization in UAV-relay-assisted networks	×	✓	×	×	8
UAV path planning	✓	×	×	✓	9
Data aggregation in UAV-assisted IoT Networks	×	✓	×	✓	10
Optimizing cost/profit function in UAV-assisted 5G networks	×	✓	×	×	11
Throughput and energy efficiency maximization for UAV-assisted vehicular networks	×	✓	×	×	13
Link coverage analysis in cellular UAV communications	✓	×	×	✓	14
UAV beam alignment in mmWave communications	✓	✓	×	×	15
Interference cancellation and sum-rate maximization for multi-beam UAVs	✓	✓	×	×	16
UAV swarm efficient trajectory	✓	✓	×	✓	17
Reliable UAV swarm under D2D communications	✓	×	×	✓	18
Design and optimization for Cellular UAV-to-X communications	✓	✓	×	✓	19
Cellular network analysis with underlay and overlay UAV-to-UAV communications	✓	×	×	✓	20
Average capacity maximization for multi-UAV coverage	×	×	×	✓	21
Completion time minimization in UAV-to-UAV communications	×	✓	×	✓	22
Air-to-air channel model for UAV communications	✓	×	×	✓	23
Joint 3d placement and multi-beam design for UAV-assisted networks	×	✓	×	×	24
Location allocation problem for UAV base station	×	✓	×	✓	25
Localization problem in UAV-assisted edge computing network	×	✓	×	✓	26
Localization and power allocation in UAV swarm network	×	✓	×	✓	27
Positioning likelihood of UAVs in 5G networks	×	✓	×	✓	28
Beam management in mmWave UAV mesh networks	✓	×	×	✓	29
Sum-rate optimization with energy-saving UAV swarm	×	✓	×	✓	30
Analytical channel models for mmWave UAV networks	✓	×	✓	✓	31
Present paper	✓	✓	✓	✓	-

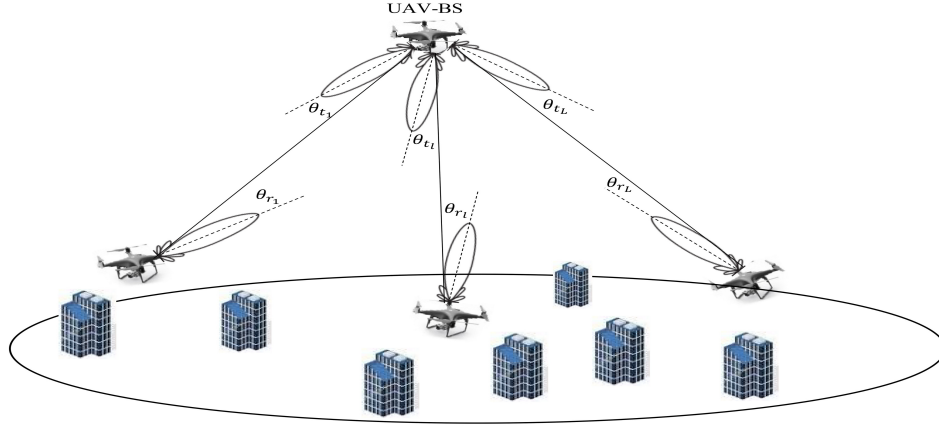


**Figure 1** Multi UAV Communication Network

To make the benefits of beamforming properties, the UAV-BS has the permission to fly in high altitude area to create LoS channel with the other users. Without loss of generality, we assume that each user's antenna is aligned towards the  $z$ -axis of the corresponding antenna in the UAV-BS and vice versa. The random physical effects of propelling rotors, controlling system faults and environmental phenomena such as air pressure could cause non-negligible fluctuations in any of the users which results in deviations of Angle of Departure (AoD) in transmitters and Angle of Arrival (AoA) in receivers. According to<sup>32,33</sup>, the PDF of these deviations could be considered as Gaussian distribution. Based on the alignment of antennas in  $z$ -axis, the AoD deviations of transmitters in UAV-BS are denoted by  $\theta_{tx_i}$  and  $\theta_{ty_i}$  in the  $x-z$  plane and  $y-z$  plane, respectively, and the AoA deviations of receivers in each user are denoted by  $\theta_{rx_i}$  and  $\theta_{ry_i}$  in the  $x-z$  plane and  $y-z$  plane, respectively. Thus, we have  $\theta_{\omega_i} \sim N(\theta'_{\omega_i}, \sigma_{\omega_i}^2)$  in which  $\omega \in \{tx, ty, rx, ry\}$  (including both transmitter and receiver sides). Since the antenna gain is assumed to be constant in  $x-z$  plane, the effect of fluctuations on the UAVs could be negligible in that dimension and we could compromise the impact of deviation in  $x-z$  plane. Hence, the antenna gain is only a function of  $\theta_{ty_i}$  and  $\theta_{ry_i}$  at each user. The summary of notations is described in Table 2.

## 2.1 | SNR Analysis under Hovering Fluctuation

The UAV-BS communicates with its users in TDMA mode and allocates the power  $P_l$  for each user at each time slot. Considering  $h_l$  as the small-scale fading over the link between  $U_l$  and UAV-BS and compromising the doppler shift effects, the received SNR could be expressed as

$$\gamma_l = \frac{|h_l|^2 P_l \mathbb{G}(\theta_{ty_l}, \theta_{ry_l})}{PL(d_l) \sigma_l^2}, \quad (1)$$

where  $\mathbb{G}(\theta_{ty_l}, \theta_{ry_l})$  is instantaneous antenna gain,  $\sigma_l^2$  indicates the variance of the Additive White Gaussian Noise (AWGN),  $h_l$  and  $PL(d_l)$  denote the channel coefficient and path loss between UAV user and UAV-BS, respectively. To make the benefits of mmWave properties, it is assumed that the altitude of UAV-BS is high enough to provide LoS link to the UAV users. Thus, considering the Rician distribution for the line of sight links between UAV-BS and the UAV users, seems reasonable and the corresponding channel gain takes the noncentral Chi-square distribution as below

$$f_{h_l^2}(\xi) = \frac{1}{2} e^{-\frac{1}{2}(\xi + k_l)} I_0(\sqrt{k_l \xi}), \quad (2)$$

where  $k_l$  represents the Rician factor and  $I_0(\cdot)$  is the modified Bessel function of the first kind and order zero.

Noting that there is no standard model for U2U communications and according to the distance between UAV-BS and UAV users, we apply the free space path loss reported by 3GPP for Urban Macrocell (UMa) scenario<sup>34</sup> as following

$$PL^{dB}(d_l) = 32.4 + 20 \log_{10} d_l + 20 \log_{10} f_c, \quad (3)$$

**Table 2** Summary of Notations

Symbols	Description
UAV-BS	UAV Base Station
$U_l$	$l$ th UAV user
$L$	Number of UAV users
$(x, y, z)$	Coordination of UAV-BS
$(x_l, y_l, z_l)$	Coordination of $U_l$
$d_l$	Distance between UAV-BS and $U_l$
$H_{min}, H_{max}$	Minimum and maximum of flight height for UAV-BS
$\theta_{txl}, \theta_{tyl}$	Angle of departure deviations of transmitters in UAV-BS
$\theta_{rxl}, \theta_{ryl}$	Angle of arrival deviations of receivers in each user
$P_l, P_{max}$	Allocated power for $U_l$ and maximum power to be allocated for $U_l$
$h_l$	Small-scale fading over the link between $U_l$ and UAV-BS
$PL(d_L)$	Free space path loss between $U_l$ and UAV-BS
$\sigma_l$	Variance of AWGN in $U_l$
$f_c$	Carrier frequency used by UAV-BS
$k_l$	Rician factor of $U_l$
$f_{h_l^2}(\xi)$	Distribution of channel gain between $U_l$ and UAV-BS
$\mathbb{G}(\theta_{tyl}, \theta_{ryl})$	Instantaneous antenna gain in the direct line
$G(\theta_{tyl}),$ $G(\theta_{ryl})$	Array gains at the transmitting antenna and the corresponding receiving UAV
$G(\theta_{\omega_l})$	Approximation of $G(\theta_{\omega_l})$ by sectorized-cosine function
$N, M$	Number of antenna elements, Number of sectors in each element
$f_{G_{\omega_l}}(w)$	PDF of $G(\theta_{\omega_l})$
$f_{G_l}(u)$	PDF of the deviation of antennas in the array factor
$\gamma_l, \gamma_0$	Received SNR at $U_l$ , SNR threshold
$f_{\gamma_l}(\gamma)$	PDF of SNR
$\mathcal{P}_l^{suc}$	Successful transmission probability for each user
$\mathcal{P}_{av}^{suc}$	Average successful transmission probability
$\alpha, \nu$ and $\lambda_l$	Lagrangian coefficients

in which  $f_c$  is the carrier frequency used by UAV-BS and  $d_l = \sqrt{(x - x_l)^2 + (y - y_l)^2 + (z - z_l)^2}$  is the distance between UAV-BS and  $l$ th UAV.

Since each antenna consists of  $N$  elements, the instantaneous antenna gain in the direct line is given by<sup>35</sup>

$$\mathbb{G}(\theta_{tyl}, \theta_{ryl}) = \underbrace{\frac{\sin^2(N\pi\theta_{tyl})}{N \sin^2(\pi\theta_{tyl})}}_{G(\theta_{tyl})} \underbrace{\frac{\sin^2(N\pi\theta_{ryl})}{N \sin^2(\pi\theta_{ryl})}}_{G(\theta_{ryl})}, \quad (4)$$

where  $G(\theta_{ly_l})$  and  $G(\theta_{ry_l})$  are the array gains at the transmitting antenna and the corresponding receiving UAV, respectively. According to<sup>31</sup>,  $G(\theta_{\omega_l})$  could be approximated by *sectorized-cosine* model as

$$G(\theta_{\omega_l}, M) \simeq \begin{cases} N \cos\left(\frac{\pi N i}{2MN}\right)^{2.5} & \frac{i}{MN} \leq |\theta_{\omega_l}| < \frac{i+1}{MN} \\ 0 & \text{otherwise} \end{cases}$$

$$= N\Pi(MN\theta_{\omega_l}) + \sum_{i=1}^{M-1} N \cos\left(\frac{\pi N i}{2MN}\right)^{2.5} \times \left[ \Pi\left(\frac{MN|\theta_{\omega_l}|}{i+1}\right) - \Pi\left(\frac{MN|\theta_{\omega_l}|}{i}\right) \right], \quad (5)$$

where  $M$  denotes the number of sectors in each element and  $\Pi(x)$  denotes the Rect. function equal to 1 for  $|x| < 1$  and zero otherwise. The PDF of  $G(\theta_{\omega_l})$  can be obtained by<sup>31</sup>

$$f_{G_{\omega_l}}(w) = \sum_{i=0}^{M-1} A_{\omega_{l,i}}(\theta'_{\omega_l}, \sigma_{\omega_l}) \delta\left(w - N \cos\left(\frac{\pi N i}{2MN}\right)^{2.5}\right), \quad (6)$$

where

$$A_{\omega_{l,i}}(\theta'_{\omega_l}, \sigma_{\omega_l}) = Q\left(\frac{i + NM\theta'_{\omega_l}}{NM\sigma_{\omega_l}}\right) - Q\left(\frac{i + 1 + NM\theta'_{\omega_l}}{NM\sigma_{\omega_l}}\right) \\ + Q\left(\frac{i - NM\theta'_{\omega_l}}{NM\sigma_{\omega_l}}\right) - Q\left(\frac{i + 1 - NM\theta'_{\omega_l}}{NM\sigma_{\omega_l}}\right) \quad (7)$$

where  $Q(\cdot)$  indicates the *Q-function*. Therefore, the PDF of the deviation of antennas in the array factor is given by

$$f_{G_l}(u) = \int_0^{\infty} \frac{1}{w} f_{G_{ly_l}}(u) f_{G_{ry_l}}\left(\frac{u}{w}\right) dw \\ = \sum_{i=0}^{M-1} \sum_{j=0}^{M-1} D_{i,j}^l \delta(u - B_{ij}(M, N)), \quad (8)$$

where  $D_{i,j}^l = A_{ly_{l,i}}(\theta'_{ly_l}, \sigma_{ly_l}) A_{ry_{l,j}}(\theta'_{ry_l}, \sigma_{ry_l})$  and  $B_{ij}(M, N) = N^2 \cos\left(\frac{\pi N i}{2MN}\right)^{2.5} \cos\left(\frac{\pi N j}{2MN}\right)^{2.5}$ . Now, we could calculate the PDF of  $\gamma_l$  as

$$f_{\gamma_l}(\gamma) = \int_0^{\infty} \frac{PL(d_l)\sigma_l^2}{P_l\xi} f_{G_l}\left(\frac{PL(d_l)\sigma_l^2\gamma}{P_l\xi}\right) f_{h_l^2}(\xi) d\xi \\ = \frac{PL(d_l)\sigma_l^2 e^{-\frac{1}{2}k_l}}{2P_l} \sum_{i=0}^{M-1} \sum_{j=0}^{M-1} D_{i,j}^l \times \\ \int_0^{\infty} \frac{e^{-\frac{1}{2}\xi} I_0(\sqrt{k_l\xi})}{\xi} \delta\left(\frac{PL(d_l)\sigma_l^2\gamma}{P_l\xi} - B_{ij}(M, N)\right) d\xi \\ = \frac{PL(d_l)\sigma_l^2 e^{-\frac{1}{2}k_l}}{2P_l} \sum_{i=0}^{M-1} \sum_{j=0}^{M-1} \frac{D_{i,j}^l}{B_{ij}(M, N)} \times e^{-\frac{PL(d_l)\sigma_l^2\gamma}{2B_{ij}(M, N)P_l}} I_0\left(\sqrt{\frac{k_l PL(d_l)\sigma_l^2\gamma}{B_{ij}(M, N)P_l}}\right), \quad (9)$$

In the next subsection, we derive the successful transmission probability regarding to the channel model obtained in current subsection.



## 2.2 | Successful Transmission Probability Analysis

The successful transmission probability for each user is calculated by

$$\begin{aligned} \mathcal{P}_l^{suc} &= \Pr\{\gamma_l \geq \gamma_0\} = \int_{\gamma_0}^{\infty} f_{\gamma_l}(\gamma) d\gamma \\ &= \frac{PL(d_l)\sigma_l^2 e^{-\frac{1}{2}k_l}}{2P_l} \sum_{i=0}^{M-1} \sum_{j=0}^{M-1} D_{i,j}^l \sum_{m=0}^{\infty} \frac{k_l^m P_l}{2^m m! \Gamma(m+1)} \times \Gamma\left(m+1, \frac{PL(d_l)\sigma_l^2 \gamma_0}{2B_{ij}(M, N)P_l}\right), \end{aligned} \quad (10)$$

where  $PL(d_l) = \beta d_l^2$  in which  $\beta = (41.68f_c)^2$  ( $f_c$  is the carrier frequency) and  $\Gamma(s, t)$  is the upper incomplete Gamma function.

We define the average successful transmission probability of the network as  $\mathcal{P}_{av}^{suc} = \frac{1}{L} \sum_{l=1}^L \mathcal{P}_l^{suc}$  and we use the expansion series instead of incomplete Gamma function as  $\Gamma(m+1, x) = m!e^{-x} \sum_{n=0}^m \frac{x^n}{n!}$ , which is given by

$$\mathcal{P}_{av}^{suc} = \frac{1}{L} \sum_{l=1}^L \sum_{i=0}^{M-1} \sum_{j=0}^{M-1} e^{-\frac{1}{2}k_l} D_{i,j}^l e^{-T_{i,j}^l} \times \sum_{m=0}^{\infty} \frac{k_l^m}{2^m \Gamma(m+1)} \sum_{n=0}^m \frac{(T_{i,j}^l)^n}{n!}, \quad (11)$$

in which  $T_{i,j}^l = \frac{\beta \sigma_l^2 \gamma_0 d_l^2}{2B_{ij}(M, N)P_l}$ . The last part of the equation (11) including two summations is rewritten as

$$\begin{aligned} \sum_{m=0}^{\infty} \frac{k_l^m}{2^m \Gamma(m+1)} \sum_{n=0}^m \frac{(T_{i,j}^l)^n}{n!} &= \left\{1 + \frac{k_l}{2^1 0!} \left[1 + \underbrace{T_{i,j}^l}_{\ll 1}\right] \right. \\ &\quad \left. + \frac{k_l^2}{2^3 2!} \left[1 + \underbrace{T_{i,j}^l + T_{i,j}^2}_{\ll 1}\right] + \frac{k_l^3}{2^4 3!} \left[1 + \underbrace{T_{i,j}^l + T_{i,j}^2 + T_{i,j}^3}_{\ll 1}\right] + \dots \right\} \\ &\geq \sum_{m=1}^{\infty} \frac{mk_l^m}{2^m \Gamma(m+1)} = S_l. \end{aligned} \quad (12)$$

The underbraced phrases in upside parts of equation (12) have been omitted to obtain its minimum amount, however, note that in practical systems with low noise variances, we have  $T_{i,j}^l \ll 1$  which makes this assumption reasonable (The numerical results also confirm this assumption in section IV). Then, the average successful transmission probability is lower bounded by

$$\mathcal{P}_{av}^{suc} \geq \frac{1}{L} \sum_{l=1}^L \sum_{i=0}^{M-1} \sum_{j=0}^{M-1} e^{-\frac{1}{2}k_l} D_{i,j}^l S_l e^{-T_{i,j}^l}. \quad (13)$$

In the next section, we will use the obtained lower bound instead of equation (11) to define the optimization problem.

## 3 | OPTIMIZING THE SUCCESSFUL TRANSMISSION PROBABILITY

Increasing the successful transmissions in the network would be taken to the account as an evaluating metric for Quality of Service (QoS). In this paper, we intend to find the best location for UAV-BS and assign the optimum power for each UAV to maximize the average successful transmission probability among the users. Thus, the optimization problem could be defined as maximizing the lower bound of the average successful transmission probability as following

$$\begin{aligned} \text{P1 : } \max_{\{P_l\}, x, y, z} & \frac{1}{L} \sum_{l=1}^L \sum_{i=0}^{M-1} \sum_{j=0}^{M-1} e^{-\frac{1}{2}k_l} D_{i,j}^l S_l e^{-T_{i,j}^l} \\ \text{St. to: } & 0 < P_l \leq P_{max}, \quad \forall l = 1, \dots, L \\ & z_l \leq z, \quad \forall l = 1, \dots, L \\ & H_{min} \leq z \leq H_{max}, \end{aligned} \quad (14)$$

where  $P_{max}$  is the maximum allowable transmission power for each UAV,  $H_{min}$  and  $H_{max}$  are the minimum and maximum altitudes for UAV-BS, respectively. Note that optimizing the altitude of UAV-BS is necessary since the altitude of other UAV

users are not equal. The first constraint guarantees that each UAV user will receive the service during each time slot. On the contrary, the plethora of the users in UAV networks causes more power consumption in the UAV-BS, therefore, the maximum assignable power for each user is bounded by  $P_{max}$ . Considering the urban environment, the LoS links would be blocked by surrounding tall buildings, hence, the second constraint would be a reasonable expression to assure the LoS channel between the UAV-BS and UAV users. The third constraint pertains to UAV limitations and implementation standards.

Generally, the objective function in the optimization problem is non-convex and is difficult to be solved directly. The phrase  $\frac{1}{L}$  is ineffective in optimization problem and could be eliminated from now on. Using the approximation  $e^{-x} \simeq 1 - x$  for  $x \ll 1$ , we approximate  $e^{-T_{i,j}^l} \simeq 1 - T_{i,j}^l$ . Substituting the amount of  $T_{i,j}^l$ , the problem P1 is equivalent to

$$\begin{aligned} \text{P2 : } & \max_{\{P_l\}, x, y, z} \sum_{l=1}^L \sum_{i=0}^{M-1} \sum_{j=0}^{M-1} e^{-\frac{1}{2}k_l} D_{i,j}^l S_l \left( 1 - \frac{\beta \sigma_l^2 \gamma_0 d_l^2}{2B_{ij}(M, N)P_l} \right) \\ \text{St. to: } & 0 < P_l \leq P_{max}, \quad \forall l = 1, \dots, L \\ & z_l \leq z, \quad \forall l = 1, \dots, L \\ & H_{min} \leq z \leq H_{max}. \end{aligned} \quad (15)$$

Maximizing the objective function in P2 is equivalent to minimizing the righthand side sentence inside the parentheses in that function. Thus, P2 is converted to

$$\begin{aligned} \text{P3 : } & \min_{\{P_l\}, x, y, z} \sum_{l=1}^L \sum_{i=0}^{M-1} \sum_{j=0}^{M-1} e^{-\frac{1}{2}k_l} D_{i,j}^l S_l \frac{\beta \sigma_l^2 \gamma_0 d_l^2}{2B_{ij}(M, N)P_l} \\ \text{St. to: } & 0 < P_l \leq P_{max}, \quad \forall l = 1, \dots, L \\ & z_l \leq z, \quad \forall l = 1, \dots, L \\ & H_{min} \leq z \leq H_{max}. \end{aligned} \quad (16)$$

Assume that we know  $(x, y, z)$ , it can be seen that the object function in problem P3 is a decreasing function in terms of  $P_l$  and the maximum amount of  $P_l^* = P_{max}$  is the solution to P3. Thus, the problem P3 is converted to

$$\begin{aligned} \text{P4 : } & \min_{x, y, z} \sum_{l=1}^L \sum_{i=0}^{M-1} \sum_{j=0}^{M-1} \frac{e^{-\frac{1}{2}k_l} D_{i,j}^l S_l \sigma_l^2 \gamma_0}{2B_{ij}(M, N)P_{max}} \\ & \times [(x - x_l)^2 + (y - y_l)^2 + (z - z_l)^2] \\ \text{St. to: } & z_l \leq z, \quad \forall l = 1, \dots, L \\ & H_{min} \leq z \leq H_{max}. \end{aligned} \quad (17)$$

$(x - x_l)^2$  is a convex function for all  $x$  and so are  $(y - y_l)^2$  and  $(z - z_l)^2$  for all  $y$  and  $z$ , respectively. Since the summation of several convex functions achieves a convex function, hence, P4 is convex and we could use the KKT conditions to obtain the optimal values for  $(x, y, z)$  by defining the Lagrangian function as below

$$\begin{aligned} \mathcal{L} = & \sum_{l=1}^L \sum_{i=0}^{M-1} \sum_{j=0}^{M-1} \frac{e^{-\frac{1}{2}k_l} D_{i,j}^l S_l \sigma_l^2 \gamma_0}{2B_{ij}(M, N)P_{max}} \times \\ & [(x - x_l)^2 + (y - y_l)^2 + (z - z_l)^2] \\ & + \alpha(z - H_{max}) + \nu(H_{min} - z) + \lambda_l(z_l - z), \end{aligned} \quad (18)$$

where  $\alpha \geq 0$ ,  $\nu \geq 0$  and  $\lambda \geq 0$  are Lagrangian coefficients. The KKT conditions are given as

$$\left\{ \begin{array}{l} \frac{\partial \mathcal{L}}{\partial x} = \sum_{l=1}^L \sum_{i=0}^{M-1} \sum_{j=0}^{M-1} \frac{e^{-\frac{1}{2}k_l} D_{i,j}^l S_l \sigma_l^2 \gamma_0}{B_{ij}(M,N) P_{max}} (x - x_l) = 0 \\ \frac{\partial \mathcal{L}}{\partial y} = \sum_{l=1}^L \sum_{i=0}^{M-1} \sum_{j=0}^{M-1} \frac{e^{-\frac{1}{2}k_l} D_{i,j}^l S_l \sigma_l^2 \gamma_0}{B_{ij}(M,N) P_{max}} (y - y_l) = 0 \\ \frac{\partial \mathcal{L}}{\partial z} = \sum_{l=1}^L \sum_{i=0}^{M-1} \sum_{j=0}^{M-1} \frac{e^{-\frac{1}{2}k_l} D_{i,j}^l S_l \sigma_l^2 \gamma_0}{B_{ij}(M,N) P_{max}} (z - z_l) + \alpha - \nu - \sum_{l=1}^L \lambda_l = 0 \\ \alpha(z - H_{max}) = 0 \\ \nu(H_{min} - z) = 0 \\ \lambda_l(z_l - z) = 0. \end{array} \right. \quad (19)$$

Based on hierarchical arrangement of UAVs and different positions for UAV users, satisfying the last phrase in equation (19) is achieved in two conditions; The first condition occurs if  $\lambda_l = 0 \forall l = 1, \dots, L$ . The second condition occurs if  $\lambda_a \neq 0$  and  $\lambda_l = 0 \forall l = 1, \dots, L \setminus a$  where  $U_a$  is the UAV user with maximum flight height ( $z_a = \max(z_l)$ ). Note that for more than one  $\lambda_l \neq 0$ , the height of UAV-BS,  $z$ , must take several values according to the last complementary slackness in equation (19), which is impossible.

In the first condition, regarding the two other complementary slackness in equation (19), we have four following cases:

Case 1)  $\alpha = 0$  and  $\nu = 0$ : the solution to the equation (19) is given by

$$x^* = \frac{\sum_{l=1}^L \sum_{i=0}^{M-1} \sum_{j=0}^{M-1} \frac{e^{-\frac{1}{2}k_l} D_{i,j}^l S_l \sigma_l^2}{B_{ij}(M,N)} x_l}{\sum_{l=1}^L \sum_{i=0}^{M-1} \sum_{j=0}^{M-1} \frac{e^{-\frac{1}{2}k_l} D_{i,j}^l S_l \sigma_l^2}{B_{ij}(M,N)}}. \quad (20)$$

$$y^* = \frac{\sum_{l=1}^L \sum_{i=0}^{M-1} \sum_{j=0}^{M-1} \frac{e^{-\frac{1}{2}k_l} D_{i,j}^l S_l \sigma_l^2}{B_{ij}(M,N)} y_l}{\sum_{l=1}^L \sum_{i=0}^{M-1} \sum_{j=0}^{M-1} \frac{e^{-\frac{1}{2}k_l} D_{i,j}^l S_l \sigma_l^2}{B_{ij}(M,N)}}. \quad (21)$$

$$z^* = \frac{\sum_{l=1}^L \sum_{i=0}^{M-1} \sum_{j=0}^{M-1} \frac{e^{-\frac{1}{2}k_l} D_{i,j}^l S_l \sigma_l^2}{B_{ij}(M,N)} z_l}{\sum_{l=1}^L \sum_{i=0}^{M-1} \sum_{j=0}^{M-1} \frac{e^{-\frac{1}{2}k_l} D_{i,j}^l S_l \sigma_l^2}{B_{ij}(M,N)}}. \quad (22)$$

Case 2)  $\alpha = 0$  and  $\nu \neq 0$ : in this case, we should have  $z = H_{min}$  to satisfy the KKT conditions and the solution to  $x^*$  and  $y^*$  are obtained by the equations (20) and (21), respectively. Note that the obtained value for  $\nu$  from the third phrase of equation (19) will be positive which is necessary for the KKT conditions.

Case 3)  $\alpha \neq 0$  and  $\nu = 0$ : in this case, we should have  $z = H_{max}$  to satisfy the KKT conditions, but substituting  $z = H_{max}$  in third phrase of equation (19) achieves a negative value for  $\alpha$  which contradicts the conditions, hence, this case is unacceptable.

Case 4)  $\alpha \neq 0$  and  $\nu \neq 0$ : to satisfy the complementary slackness in equation (19), we should have simultaneously  $z = H_{max}$  and  $z = H_{min}$ , which is impossible. Therefore, this case is not a solution for problem.

In the second condition, the height of UAV-BS,  $z$  takes the maximum value of  $z_l$ , since it has to be higher than all UAV users, that is  $z = z_a$ . Therefore, having  $\alpha \neq 0$  or  $\nu \neq 0$  implies that  $z = H_{max}$  or  $z = H_{min}$ , respectively, which is contradictory to  $z = z_a$  and we should have  $\alpha = 0$  or  $\nu = 0$ . Then, the amount of  $x^*$  and  $y^*$  are obtained by the equations (20) and (21), respectively. Also,  $\lambda_a$  could be found from the third phrase in equation (19), which yields a positive value.

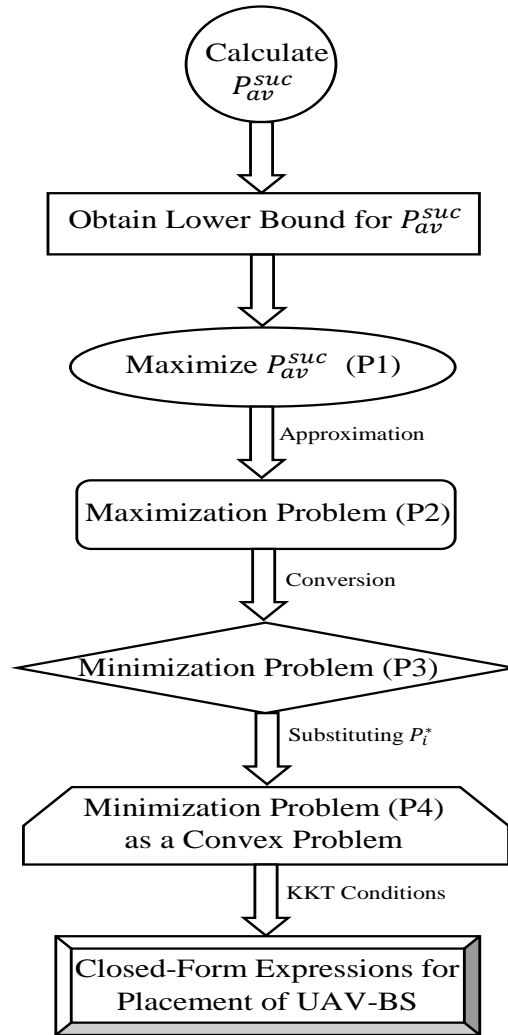


**Figure 2** The Process of Solving the Optimization Problem

The optimal solution to the problem P4, is found by testing the solutions of case 1 and case 2 in the condition 1 and also the condition 2, to determine which set of the answers maximizes the average successful transmission probability. The process of approximation, conversion and solution to the optimization problem would be summarized in Figure 2.

## 4 | NUMERICAL RESULTS

In this section, we perform Monte-Carlo simulations to evaluate the analytical results. To simulate an actual antenna gain corresponding to the equation (4), we generate  $10^6$  independent random variables for  $\theta_{\omega_i}$  using a given Normal distribution  $(N(\theta'_{\omega_i}, \sigma_{\omega_i}^2))$ , without loss of generality, we assume that  $\theta'_{\omega_i}$  and  $\sigma_{\omega_i}$  are equal for all UAV users in our simulations. Then, we generate  $10^6$  independent channel coefficients from a Rician distribution to simulate the small scale fading. Thus,  $10^6$  values of received SNR on each user could be obtained to be compared with  $\gamma_0$ . Then, we distribute the UAV users in a  $1000^m \times 1000^m$  square area which is divided into equal  $L$  regions so that at least one UAV user is located in each region randomly in the Cartesian coordination. This consideration is not specific and it is provided for a better realization of UAV-BS location, i.e. the simulation for a dense aggregation of UAVs in a given area is similar to the simulation of sparse distribution of UAVs. Likewise, the Rician factor has been considered equal for the UAV users in some diagrams to ease the calculations and considering various

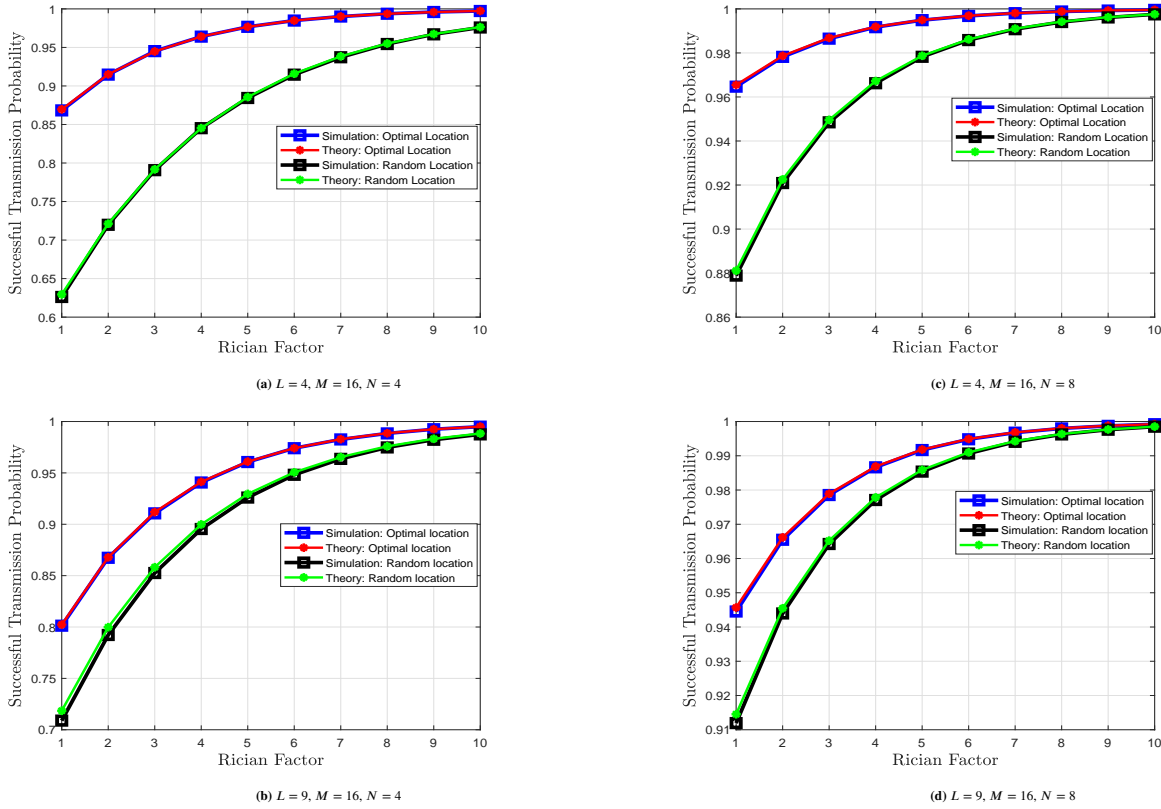


**Figure 3** Average Probability of Successful Transmission vs.  $k_l$

values, does not have a significant impact on proceeding of the results. The settings are as follows:  $f_c = 6GHz$ ,  $M = 16$ ,  $\sigma^2 = -90dBm$ ,  $H_{min} = 150m$  and  $\gamma_0 = 1$ . The rest of the parameters varies for each diagram to obtain various results. Also, the simulations take place for  $L = 4$  and  $L = 9$  UAV users and the results are derived for optimum and random placement of the main UAV. Finally, a set of diagrams are juxtaposed in each figure for better observations.

Figure 3 shows  $\mathcal{P}_{av}^{suc}$  vs. Rician factor considering equal to  $k_l$  for each UAV. The Figures 3a and 3c are achieved for  $L = 4$  and the Figures 3b and 3d are achieved for  $L = 9$ . As seen in the figures, the simulation results verify the analytical results both in optimal approach and random localization of UAV-BS, precisely. As expected, all diagrams show that increasing the Rician factor causes more successful transmissions. The reason to this behavior is due to improvement of channel quality for higher amounts of Rician factor which causes less errors during the transmissions. In addition, the diagrams demonstrate the effect of number of antenna elements ( $N$ ) in the successful transmissions for  $N = 4$  and  $N = 8$ . The Figures 3a and 3b are achieved for  $N = 4$  while the Figures 3c and 3d are obtained for  $N = 8$ . According to the equation (4), as  $N$  increases, the channel gain corresponding to the mmWave communications increases in the direct link, that is, increasing the number of antenna elements ( $N$ ), increases  $\mathcal{P}_{av}^{suc}$  which is obvious in the diagrams. To show the effectiveness of the proposed optimal solution, we compare our results with random location of UAV-BS so that a random location of the main UAV results in lower successful transmissions and confirms the superiority of our method for various conditions.

Figure 4 is the exhibition of  $\mathcal{P}_{av}^{suc}$  vs. maximum allocated power for each UAV. The Figures 4a and 4c are achieved for  $L = 4$  and the Figures 4b and 4d are achieved for  $L = 9$ . As expected, allocating more power for each UAV would enhance the received signal power in the destination and consequently increases  $\mathcal{P}_{av}^{suc}$ . Similar to the Figure 3, we show the effects of  $N$  for different number of UAVs and various location of UAV-BS. The Figures 4a and 4b are delineated for  $N = 4$  and the Figures 4c and 4d are exhibited for  $N = 8$ , respectively. As discussed above, increasing the number of antenna elements would enhance the successful transmission while  $P_{max}$  varies in the value. Likewise, the optimum value for the main UAV location achieves maximum successful transmissions rather than random location which shows the superiority of our proposed approach.

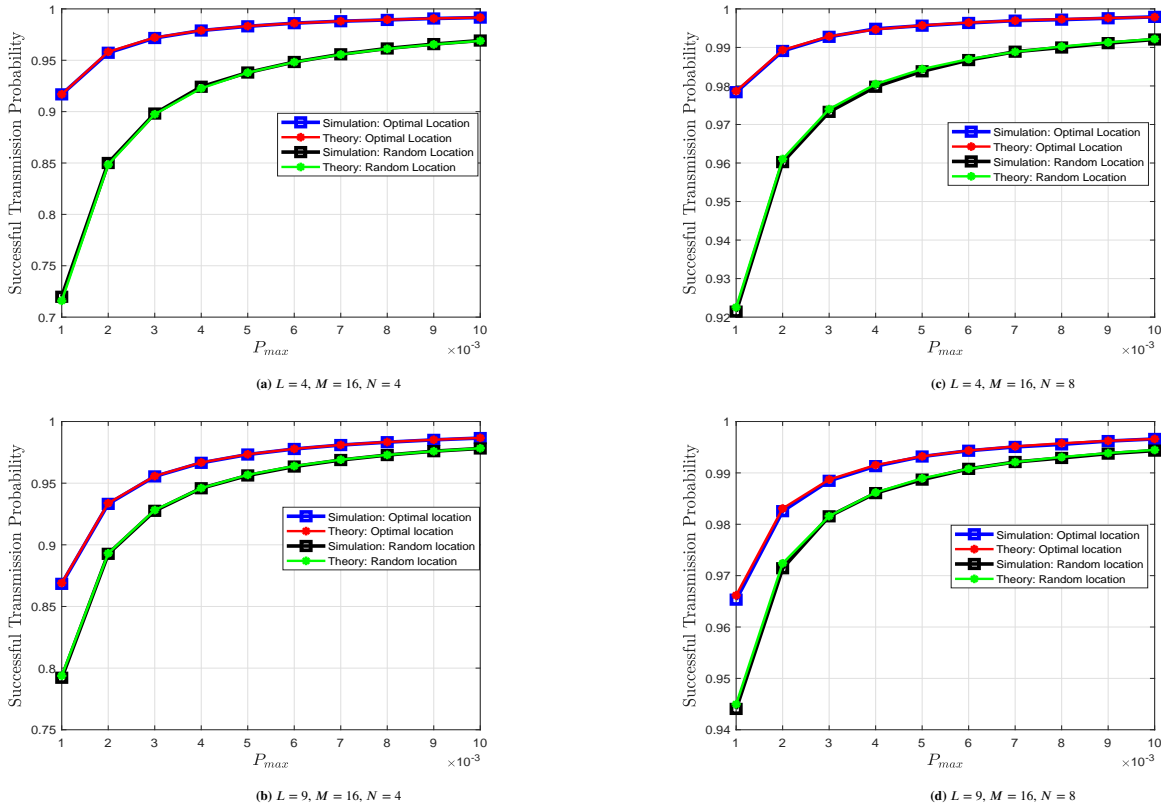


**Figure 4** Average Probability of Successful Transmission vs.  $P_{max}$  for ( $k_l = 2$ )

Figure 5 demonstrates  $\mathcal{P}_{av}^{suc}$  vs. variance of fluctuations ( $\sigma_{\omega_l}$ ) which is highly related to the environmental affects on the UAVs. The Figures 5a and 5c are achieved for  $L = 4$  and the Figures 5b and 5d are achieved for  $L = 9$ . The high  $\sigma_{\omega_l}$  causes the higher divergence in the arrival and departure angles of transmitter and receiver which reduces the advantages of direct link between them. Hence, as  $\sigma_{\omega_l}$  increases, the antenna gains decrease in both transmitting and receiving UAVs which reduces the received SNR at the UAVs and as a result decreases  $\mathcal{P}_{av}^{suc}$ . Similar to the previous figures, the effect of  $N$  has been demonstrated in the diagrams, as well. The higher successful transmissions are achieved by growth of number of antenna elements even for intense fluctuations. Likewise, the proposed method for UAV-BS placement outperforms the UAV-BS random location.

Finally, Figure 6 is the 3D demonstration of  $\mathcal{P}_{av}^{suc}$  for a non-Uniform distribution of UAVs in which the UAVs have been considered close to each other in  $x - y$  plane in a specific area. The colorful diagram represents the simulation results, achieved for each point in the area and the green point is the optimal point of  $\mathcal{P}_{av}^{suc}$  achieved by lower bound approach which verifies the simulation results and confirms our calculations.

Note that the UAVs have been distributed randomly and the amount of  $\mathcal{P}_{av}^{suc}$  for  $L = 4$  is greater than that of  $L = 9$ , but it does not necessarily mean that reducing the number of UAVs will increase the successful transmissions, because  $\mathcal{P}_{av}^{suc}$  depends on the location of UAVs in the given area and in our simulations the location of UAVs have been closer to each other in  $L = 4$  rather than  $L = 9$ . The gap for  $\mathcal{P}_{av}^{suc}$  between random location of the main UAV and its optimum point for  $L = 4$  is greater than  $L = 9$  due to better position of UAV location in  $L = 9$  in proportion to  $L = 4$ , as well.

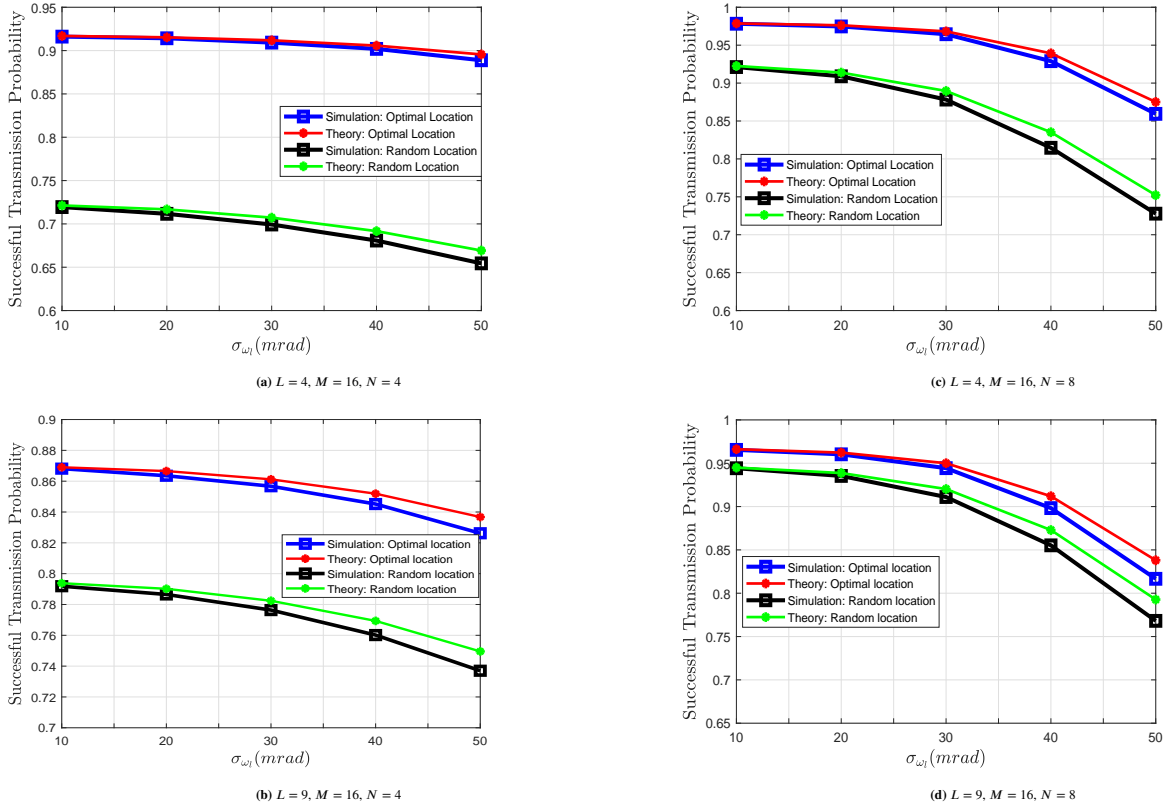


**Figure 5** Average Probability of Successful Transmission vs.  $\sigma_{\omega_l}$  for ( $k_l = 2$  and  $P_{max} = 0d Bm$ )

## 5 | CONCLUSIONS

We have investigated a downlink hierarchical UAV network in which a main UAV serves the other UAVs as users in orthogonal channels. The UAVs could use beamforming properties to increase the antenna gains. The received SNR in each UAV, is influenced by physical fluctuations both in the transmitting and receiving sides. The successful transmission probability for each link, has been obtained under Rician fading and the average successful transmission probability of the network has been derived as closed form expressions. Then, an optimization problem has been defined to maximize the average successful transmission probability in the network which is a non-convex problem. A lower bound for the average successful transmission probability was used to find an equivalent problem which was simplified with some approximations. Converting the problem into a convex problem, resulted in the optimum placement of the main UAV. The analytical results were verified by simulation results and outperformed the other methods.

Having the knowledge on the physical distribution of UAV users such as Poisson Point Process (PPP) models instead of the information about their exact locations, would be considered as an extension to the present work. Furthermore, the effect of interferences caused by the other users in non-orthogonal channels and finding the optimum trajectory for non-rotary wing UAVs will be considered in the future works.

## ACKNOWLEDGMENTS

No acknowledgment.

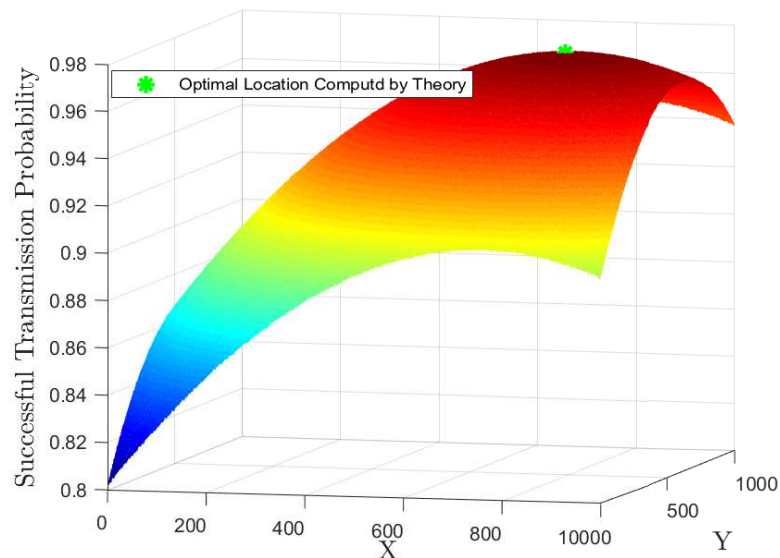


**Figure 6** Probability of Successful Transmission vs. Location of UAV

### Author contributions

All the authors have participated in preparing the article.

### Financial disclosure

None reported.

### Conflict of interest

The authors declare that they have no financial and personal relationships with other people or organizations that can inappropriately influence our work, there is no professional or other personal interest of any nature or kind in any product, service and/or company that could be construed as influencing the position presented in, or the review of this manuscript.

### SUPPORTING INFORMATION

There is no available supporting information.

### References

1. Mohammed I, Collings IB, Hanly SV. A new connectivity model for unmanned aerial vehicle communications and flying height optimization. *Transactions on Emerging Telecommunications Technologies*; n/a(n/a): e4767. doi: <https://doi.org/10.1002/ett.4767>
2. Sekander S, Tabassum H, Hossain E. Multi-Tier Drone Architecture for 5G/B5G Cellular Networks: Challenges, Trends, and Prospects. *IEEE Communications Magazine* 2018; 56(3): 96-103. doi: 10.1109/MCOM.2018.1700666
3. Zhang Z, Xiao Y, Ma Z, et al. 6G Wireless Networks: Vision, Requirements, Architecture, and Key Technologies. *IEEE Vehicular Technology Magazine* 2019; 14(3): 28-41. doi: 10.1109/MVT.2019.2921208



4. Mozaffari M, Saad W, Bennis M, Nam YH, Debbah M. A Tutorial on UAVs for Wireless Networks: Applications, Challenges, and Open Problems. *IEEE Communications Surveys Tutorials* 2019; 21(3): 2334-2360. doi: 10.1109/COMST.2019.2902862
5. Zhang H, Li X. Directional antennas modelling and coverage analysis for UAV networks with blockage effects in urban environment. *Transactions on Emerging Telecommunications Technologies* 2023; 34(4): e4737. doi: <https://doi.org/10.1002/ett.4737>
6. Zhang L, Zhao H, Hou S, et al. A Survey on 5G Millimeter Wave Communications for UAV-Assisted Wireless Networks. *IEEE Access* 2019; 7: 117460-117504. doi: 10.1109/ACCESS.2019.2929241
7. Feng W, Wang J, Chen Y, Wang X, Ge N, Lu J. UAV-Aided MIMO Communications for 5G Internet of Things. *IEEE Internet of Things Journal* 2019; 6(2): 1731-1740. doi: 10.1109/JIOT.2018.2874531
8. Na Z, Mao B, Shi J, Wang J, Gao Z, Xiong M. Joint trajectory and power optimization for UAV-relay-assisted Internet of Things in emergency. *Physical Communication* 2020; 41: 101100. doi: <https://doi.org/10.1016/j.phycom.2020.101100>
9. Shi L, Xu S, Liu H, Zhan Z. QoS-Aware UAV Coverage path planning in 5G mmWave network. *Computer Networks* 2020; 175: 107207. doi: <https://doi.org/10.1016/j.comnet.2020.107207>
10. Wang X, Garg S, Lin H, Kaddoum G, Hu J, Alhamid MF. An Intelligent UAV based Data Aggregation Algorithm for 5G-enabled Internet of Things. *Computer Networks* 2021; 185: 107628. doi: <https://doi.org/10.1016/j.comnet.2020.107628>
11. Cao H, Hu Y, Yang L. Towards intelligent virtual resource allocation in UAVs-assisted 5G networks. *Computer Networks* 2021; 185: 107660. doi: <https://doi.org/10.1016/j.comnet.2020.107660>
12. Ullah Z, Al-Turjman F, Moatasim U, Mostarda L, Gagliardi R. UAVs joint optimization problems and machine learning to improve the 5G and Beyond communication. *Computer Networks* 2020; 182: 107478. doi: <https://doi.org/10.1016/j.comnet.2020.107478>
13. Bian H, Dai H, Yang L. Throughput and energy efficiency maximization for UAV-assisted vehicular networks. *Physical Communication* 2020; 42: 101136. doi: <https://doi.org/10.1016/j.phycom.2020.101136>
14. Azari MM, Geraci G, Garcia-Rodriguez A, Pollin S. Cellular UAV-to-UAV Communications. In: ; 2019: 1-7
15. Zhang W, Zhang W, Wu J. UAV Beam Alignment for Highly Mobile Millimeter Wave Communications. *IEEE Transactions on Vehicular Technology* 2020; 69(8): 8577-8585. doi: 10.1109/TVT.2020.2997740
16. Liu L, Zhang S, Zhang R. Multi-Beam UAV Communication in Cellular Uplink: Cooperative Interference Cancellation and Sum-Rate Maximization. *IEEE Transactions on Wireless Communications* 2019; 18(10): 4679-4691. doi: 10.1109/TWC.2019.2926981
17. Shao S, He C, Zhao Y, Wu X. Efficient Trajectory Planning for UAVs Using Hierarchical Optimization. *IEEE Access* 2021; 9: 60668-60681. doi: 10.1109/ACCESS.2021.3073420
18. Han Y, Liu L, Duan L, Zhang R. Towards Reliable UAV Swarm Communication in D2D-Enhanced Cellular Networks. *IEEE Transactions on Wireless Communications* 2021; 20(3): 1567-1581. doi: 10.1109/TWC.2020.3034457
19. Zhang S, Zhang H, Di B, Song L. Cellular UAV-to-X Communications: Design and Optimization for Multi-UAV Networks. *IEEE Transactions on Wireless Communications* 2019; 18(2): 1346-1359. doi: 10.1109/TWC.2019.2892131
20. Azari MM, Geraci G, Garcia-Rodriguez A, Pollin S. UAV-to-UAV Communications in Cellular Networks. *IEEE Transactions on Wireless Communications* 2020; 19(9): 6130-6144. doi: 10.1109/TWC.2020.3000303
21. Chen R, Li X, Sun Y, Li S, Sun Z. Multi-UAV Coverage Scheme for Average Capacity Maximization. *IEEE Communications Letters* 2020; 24(3): 653-657. doi: 10.1109/LCOMM.2019.2962774
22. Wang H, Wang J, Ding G, Chen J, Yang J. Completion Time Minimization for Turning Angle-Constrained UAV-to-UAV Communications. *IEEE Transactions on Vehicular Technology* 2020; 69(4): 4569-4574. doi: 10.1109/TVT.2020.2976938

23. Ma Z, Ai B, He R, Wang G, Niu Y, Zhong Z. A Wideband Non-Stationary Air-to-Air Channel Model for UAV Communications. *IEEE Transactions on Vehicular Technology* 2020; 69(2): 1214-1226. doi: 10.1109/TVT.2019.2961178
24. Duan X, Ao S, Feng W, Tang J, Hu J. Joint 3D placement and multi-beam design for UAV-assisted wireless power transfer networks. *Physical Communication* 2021; 44: 101234. doi: <https://doi.org/10.1016/j.phycom.2020.101234>
25. Cicek CT, Gultekin H, Tavli B. The location-allocation problem of drone base stations. *Computers and Operations Research* 2019; 111: 155-176. doi: <https://doi.org/10.1016/j.cor.2019.06.010>
26. Xu F, Zhang Z, Feng J, Qin Z, Xie Y. Efficient deployment of multi-UAV assisted mobile edge computing: A cost and energy perspective. *Transactions on Emerging Telecommunications Technologies* 2022; 33(5): e4453. doi: <https://doi.org/10.1002/ett.4453>
27. Liu T, Zhao H, Yang H, Zheng K, Chatzimisios P. Design and implementation of a novel real-time unmanned aerial vehicle localization scheme based on received signal strength. *Transactions on Emerging Telecommunications Technologies* 2021; 32(11): e4350. doi: <https://doi.org/10.1002/ett.4350>
28. Sharma V, Jayakody DNK, Srinivasan K. On the positioning likelihood of UAVs in 5G networks. *Physical Communication* 2018; 31: 1-9. doi: <https://doi.org/10.1016/j.phycom.2018.08.010>
29. Zhou P, Fang X, Fang Y, He R, Long Y, Huang G. Beam Management and Self-Healing for mmWave UAV Mesh Networks. *IEEE Transactions on Vehicular Technology* 2019; 68(2): 1718-1732. doi: 10.1109/TVT.2018.2890152
30. Zhang X, Duan L. Energy-Saving Deployment Algorithms of UAV Swarm for Sustainable Wireless Coverage. *IEEE Transactions on Vehicular Technology* 2020; 69(9): 10320-10335. doi: 10.1109/TVT.2020.3004855
31. Dabiri MT, Safi H, Parsaeefard S, Saad W. Analytical Channel Models for Millimeter Wave UAV Networks Under Hovering Fluctuations. *IEEE Transactions on Wireless Communications* 2020; 19(4): 2868-2883. doi: 10.1109/TWC.2020.2968530
32. Dabiri MT, Sadough SMS, Ansari IS. Tractable Optical Channel Modeling Between UAVs. *IEEE Transactions on Vehicular Technology* 2019; 68(12): 11543-11550. doi: 10.1109/TVT.2019.2940226
33. Dabiri MT, Rezaee M, Yazdani V, Maham B, Saad W, Hong CS. 3D Channel Characterization and Performance Analysis of UAV-Assisted Millimeter Wave Links. *IEEE Transactions on Wireless Communications* 2021; 20(1): 110-125. doi: 10.1109/TWC.2020.3023477
34. 3GPP . 3rd Generation Partnership Project; Technical Specification Group Radio Access Network; Study on channel model for frequencies from 0.5 to 100 GHz. Tech. Rep. 38.901, 3rd Generation Partnership Project (3GPP); 2019. Version 16.1.0.
35. Balanis CA. *Antenna theory: analysis and design*. Wiley-Interscience . 2005.
36. Gradshteyn IS, Ryzhik IM. *Table of integrals, series, and products*. Academic press . 2014.

## AUTHOR BIOGRAPHY



**Hosein Azarhava.** received his B.Sc. and M.Sc. from university of Tabriz, Tabriz, Iran. Currently, he is pursuing the Ph.D. degree with University of Tabriz, and is a member of Wireless Laboratory (WiLab) of Faculty of Electrical and Computer Engineering in University of Tabriz. His research interests include digital communications, wireless communication networks, and wireless sensor networks.



**Mehran Pourmohammad Abdollahi** received his B.Sc. and M.Sc. from university of Tabriz, Tabriz, Iran. Currently, he is pursuing the Ph.D. degree with University of Tabriz, and is a member of Wireless Laboratory (WiLab) of Faculty of Electrical and Computer Engineering in University of Tabriz. His research interests include wireless communication networks, wireless sensor networks and cognitive radio networks.



**Javad Musevi Niya** was born in Ahar, Iran. He received his B.Sc. degree from the University of Tehran and his M.Sc. and Ph.D. Degrees both in telecommunication engineering from Sharif University of Technology (SUT) and the University of Tabriz, respectively. Since September 2006, he has been with the Faculty of Electrical and Computer Engineering of the University of Tabriz, where he is currently an Associate Professor. His current research interests include wireless communication systems, wireless sensor networks, multimedia networks and signal processing for communication systems and networks.

